The 1,800-year oceanic tidal cycle: A possible cause of rapid climate change

Charles D. Keeling* and Timothy P. Whorf

Scripps Institution of Oceanography, University of California, San Diego, La Jolla, CA 92093-0244

Contributed by Charles D. Keeling, February 2, 2000

Variations in solar irradiance are widely believed to explain climatic change on 20,000- to 100,000-year time-scales in accordance with the Milankovitch theory of the ice ages, but there is no conclusive evidence that variable irradiance can be the cause of abrupt fluctuations in climate on time-scales as short as 1,000 years. We propose that such abrupt millennial changes, seen in ice and sedimentary core records, were produced in part by well characterized, almost periodic variations in the strength of the global oceanic tide-raising forces caused by resonances in the periodic motions of the earth and moon. A well defined 1,800-year tidal cycle is associated with gradually shifting lunar declination from one episode of maximum tidal forcing on the centennial time-scale to the next. An amplitude modulation of this cycle occurs with an average period of about 5,000 years, associated with gradually shifting separation-intervals between perihelion and syzygy at maxima of the 1,800-year cycle. We propose that strong tidal forcing causes cooling at the sea surface by increasing vertical mixing in the oceans. On the millennial time-scale, this tidal hypothesis is supported by findings, from sedimentary records of ice-rafting debris, that ocean waters cooled close to the times predicted for strong tidal forcing.

High resolution ice-core and deep-sea sediment-core records over the past million years show evidence of abrupt changes in climate superimposed on slow alternations of ice-ages and interglacial warm periods. In general these abrupt changes are spaced irregularly, but a distinct subset of recurring cold periods, on the millennial time-scale, appears to be almost periodic. Such events, however, are not clearly apparent in ice-core data after the termination of the most recent glaciation, about eleven thousand years (11 kyr) BP (kyr before A.D. 2000). This absence of recent events has led to the hypothesis that their underlying cause is related to internal ice-sheet dynamics (ref. 1, p. 35). Interpretations of sediment-cores by Bond *et al.* (1, 2) indicate, however, that a 1- to 2-kyr periodicity persisted almost to the present, characterized by distinct cooling events, including the Little Ice Age that climaxed near A.D. 1600. Although evidence that cooling was more intense during glacial times may be explained by some aspect of ice-dynamics, a continuation of cooling events throughout the postglacial Holocene era suggests an alternative underlying mechanism.

The 1- to 2-kyr Ice-Rafted Debris (IRD) Cycle. In a comprehensive comparison of ice-core and sediment-core data, Bond *et al.* (1) found persistent episodic cooling events recorded as increases in the amounts of IRD in deep sea sediments of the North Atlantic Ocean basin over the past 80 kyr. Consistent periodicity was demonstrated by averaging the times between inferred cool events over 12-kyr time intervals. This "pacing" of events was found to be restricted to a narrow range between 1,328 and 1,795 years, with a grand average of 1,476 ± 585 yr, that they termed a "1–2 kyr climate cycle."

Similar to these oceanic cooling events, but less frequent and regular, are Dansgaard/Oeschger events seen in $^{18}O/^{16}O$ data of glacial ice. Although sudden warming events are more conspicuous, these data also show cooling events. Bond *et al.* (1) found that Dansgaard/Oeschger cooling events coincide with nearly every IRD event during Stage 3 of the last glaciation when Dansgaard/Oeschger events were best developed (ref. 1, p. 51). They also found that Heinrich events, massive discharges of icebergs at intervals of 6–9 kyr in the North Atlantic Ocean, were in most cases preceded by IRD events by 0.5 and 1 kyr (ref. 1, p. 48), suggesting a close link between the two phenomena.

Bond *et al.* (1) proposed "that the millennial scale climate variability documented in Greenland ice cores and North Atlantic sediments through the last glaciation was not forced by ice sheet instabilities, but instead arose through modulation of a pervasive 1–2 kyr cycle. The persistence of the cycle through virtually the entire 80 kyr record points to a single forcing mechanism that operated independently of the glacial-interglacial climate states" (ref. 1, p. 55). They did not, however, propose a specific mechanism.

The IRD events identified by Bond *et al.* (1, 2) show high spectral power density in a broad band centered at about 1,800 years (0.55 ± 0.15 cycles/kyr). The authors do not explain why this period is so much larger than the 1,476-year average pacing of cool events, but the time-distribution of pacing (ref. 1, Fig. 6*c*; G. Bond, private communication) suggests that a majority of the events were about 2,000 years apart, with occasional additional events occurring about half-way between, evidently too infrequent to cancel out a dominant spectral peak near 1,800 years. Bond *et al.* (2) in addition found a spectral peak near 5,000 years whose possible cause was also not explained. We now propose an oceanic tidal mechanism that may explain the basis for both of these spectral peaks, consistent with the actual times of IRD events.

A Proposed Tidal Mechanism for Periodic Oceanic Cooling. In a previous study (3) we proposed a tidal mechanism to explain approximately 6- and 9-year oscillations in global surface temperature, discernable in meteorological and oceanographic observations. We first briefly restate this mechanism. The reader is referred to our earlier presentation for more details. We then invoke this mechanism in an attempt to explain millennial variations in temperature.

We propose that variations in the strength of oceanic tides cause periodic cooling of surface ocean water by modulating the intensity of vertical mixing that brings to the surface colder water from below. The tides provide more than half of the total power for vertical mixing, 3.5 terawatts (4), compared with about 2.0 terawatts from wind drag (3), making this hypothesis plausible. Moreover, the tidal mixing process is strongly nonlinear, so that vertical mixing caused by tidal forcing must vary in intensity interannually even though the annual rate of power generation is constant (3). As a consequence, periodicities in strong forcing, that we will now characterize by identifying the peak forcing

Abbreviations: kyr, 1,000 years; IRD, ice-rafted debris.

*To whom reprint requests should be addressed. Email: cdkeeling@ucsd.edu.

The publication costs of this article were defrayed in part by page charge payment. This article must therefore be hereby marked "*advertisement*" in accordance with 18 U.S.C. §1734 solely to indicate this fact.

Article published online before print: *Proc. Natl. Acad. Sci. USA*, 10.1073/pnas.070047197. Article and publication date are at www.pnas.org/cgi/doi/10.1073/pnas.070047197

Table 1. Periods of revolution of the sun and moon contributing to the timing of tidal forcing

Name	Period, days	
Synodic month	29.530589	Ref. 5, p. 126
Anomalistic month	27.554551	Ref. 5, p. 131
Nodical month	27.212220	Ref. 5, p. 126
Tropical year*	365.24219879	Ref. 5, p. 125
Anomalistic year	365.25964134	Ref. 5, p. 125

*Same as ''year'' in text, equal to the average calendar year.

events of sequences of strong tides, may so strongly modulate vertical mixing and sea-surface temperature as to explain cyclical cooling even on the millennial time-scale.

As a measure of the global tide raising forces (ref. 5, p. 201.33), we adopt the angular velocity, γ, of the moon with respect to perigee, in degrees of arc per day, computed from the known motions of the sun, moon, and earth. This angular velocity, for strong tidal events, from A.D. 1,600 to 2,140, is listed in a treatise by Wood (ref. 5, Table 16). We extended the calculation of γ back to the glacial age by a multiple regression analysis that related Wood's values to four factors that determine the timing of strong tides: the periods of the three lunar months (the synodic, the anomalistic, and the nodical), and the anomalistic year, defined below. Our computations of γ first assume that all four of these periods are invariant, with values appropriate to the present epoch, as shown in Table 1. We later address secular variations. Although the assumption of invariance is a simplification of the true motions of the earth and moon, we have verified that this method of computing γ (see Table 2) produces values nearly identical to those listed by Wood, the most serious shortcoming being occasional shifts of 9 or 18 years in peak values of γ.

A time-series plot of Wood's values of γ (Fig. 1) reveals a complex cyclic pattern. On the decadal time-scale the most important periodicity is the Saros cycle, seen as sequences of events, spaced 18.03 years apart. Prominent sequences are made obvious in the plot by connected line-segments that form a series of overlapping arcs. The maxima, labeled A, B, C, D, of the most prominent sequences, all at full moon, are spaced about 180 years apart. The maxima, labeled a, b, c, of the next most prominent sequences, all at new moon, are also spaced about 180 years apart. The two sets of maxima together produce strong tidal forcing at approximately 90-year intervals.

As an indication that tidal forcing might influence temperature, Keeling and Whorf (3) found that times of cool surface temperature, on pentadal to decadal time-scales, tended to occur

Table 2. Computation of angular velocity of moon at syzygy, γ

To compute γ we employ the expression:

$$\gamma = \gamma_m - \Sigma a_i |f_i|$$

where, for full moon and new moon, respectively:

γ_m = 17.1650, 17.1489 deg·day^{-1}
a_1 = 0.002326, 0.001663 deg·day^{-1}·hr^{-1}
a_2 = 0.007372, 0.006742 deg·day^{-1}
a_3 = 0.09323, 0.08706 deg·day^{-1}
$f_1 = 0.4508\ \Delta T_{perig} - 1.4505 - 0.0254\ \Delta T_{perih}$
$f_2 = 4.8254 \sin(2\pi\ \Delta T_{node}/(24.)(27.212220)) - 0.06545$
$f_3 = (1 - \cos(2\pi\ \Delta T_{perih}/365.))$

where ΔT_{perig} (in hours), ΔT_{node} (in hours), and ΔT_{perih} (in days) are, respectively, the separation-intervals of syzygy from perigee, lunar node, and perihelion.

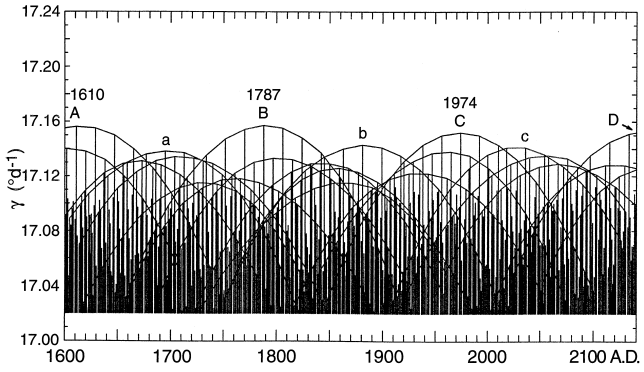

Fig. 1. Varying strength in an estimate of the tide raising forces, derived from Wood (ref. 5, Table 16). Each event, shown by a vertical line, gives a measure of the forcing in terms of the angular velocity of the moon, γ, in arc degrees per day, at the time of the event. Arcs connect events of strong 18.03-year tidal sequences. Centennial maxima are labeled, with the final one, ''D'', occurring in A.D. 2151.

at 9-year intervals near events b and C of Fig. 1: thus, at times of strong 18.03-year Saros cycle tidal events. They occurred, however, at 6-year intervals midway between events b and C, when the Saros cycle events were weak and 6-year tidal forcing was more prominent than 9-year forcing. They also noted a general tendency for interdecadal warming near 1930, when Saros cycle forcing was weak, and a lack of warming when this forcing was strong near 1880 and 1970, as though cooling near times of strong forcing lingered for several decades, despite the identified events being only single tides.

The 1,800-Year Tidal Cycle. When the time-interval of computed strong global tidal forcing is extended to include all events from 500 B.C. to A.D. 4000 (Fig. 2), two longer periodicities become evident, defined by extensions of the maxima, labeled A–D and a–c, as in Fig. 1. First, near the beginning and end of the 4,000 years plotted, every second 180-year maximum is stronger, producing a periodicity of about 360 years. More striking is a well defined millennial cycle with maxima at 398 B.C., A.D. 1425, and A.D. 3107. The latter maximum is almost matched in strength, however, by one in A.D. 3452 such that a lesser intermediate event in A.D. 3248 appears to define the repeat period of the

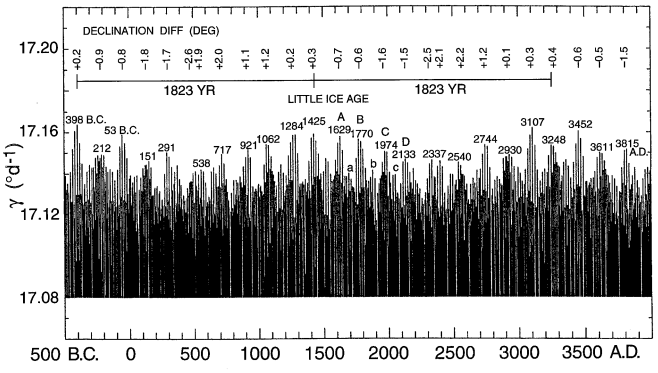

Fig. 2. Extension of Fig. 1 to illustrate millennial periodicity in tide raising forces since 500 B.C. The angular velocity, γ, was computed from functions listed in Table 2. Events of a 180-year cycle, all at full moon, are labeled with times of occurrence (B.C. or A.D.). The 1,800-year cycle is evident as a progression of solar-lunar declination difference, listed at the top of the figure in degrees of arc of the moon above (or below) the ecliptic.

GEOPHYSICS

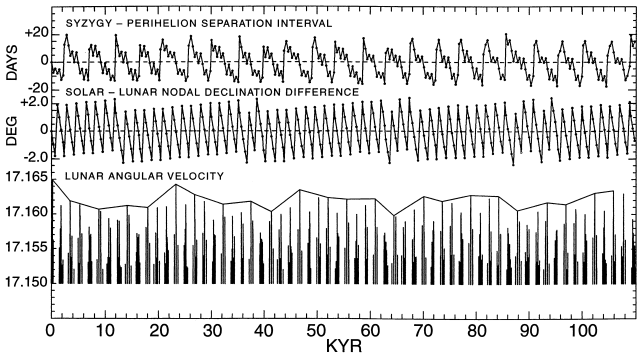

Fig. 3. Varying strength of the global tide raising forces (bottom plot), as in Figs. 1 and 2, together with parameters (top and middle plots) that reveal the basis for the 1,800- and 5,000-year tidal cycles, as described in the text. The plots are for a hypothetical 110-kyr sequence of tidal events beginning with the moon, sun, and earth in perfect alignment and closest approach (zero separation-intervals), producing a maximum γ of 17.165° per day never again attained. Tidal events occurring near peaks in the 5,000-year cycle (near zero crossings of top plot) are connected by straight lines to reveal their pattern (which includes a 23-kyr cycle not discussed in the text).

cycle as 1,823 years. The actual maximum in A.D. 3107, however, would define an interval of only 1,682 years.

The existence of tidal forcing at intervals of about 1,800 years was proposed by Otto Petersson in 1914 and 1930 [cited by Lamb (ref. 6, p. 220)]. Cartwright (7) identified events similar to those plotted in Fig. 2, consisting of strong tidal forcing 93 years apart from A.D. 1340 to 1619 and again from 3182 to 3461: thus, an average interval between clusters of 1,842 years. Keeling and Whorf (3) briefly discussed the astronomical basis for an 1,800-year tidal cycle. Computations of γ over many millennia show this 1,800-year cycle and demonstrate that the spacing of maximum events is irregular. As we will show next, the cycle is well defined, however, with an exact average period when computed for the present epoch.

The greatest possible astronomical tide raising forces would occur if the moon and the sun were to come into exact mutual alignment with the earth at their closest respective distances (7). If we only consider motions as they exist today (the present epoch) we can determine departures from this reference event as simple functions of the separation-intervals between four orbital conditions that determine these alignments and distances. The most critical condition is closeness in time to syzygy, a term that refers to either new moon or full moon. The return period of either lunar phase defines the 29.5-day synodic month. Maxima in tidal strength occur at both new and full moon: i.e., "fortnightly."

The next most critical condition of tidal forcing is the closeness of the moon to perigee, the point of the moon's elliptical orbit closest to the earth. The fortnightly tides vary in strength as a function of the time-separation of perigee and syzygy. The moon is at perigee on average once every 27.6-day anomalistic month. When it is close to both perigee and syzygy, perigean tides occur. For each moon, new or full, this happens on average every 411.78 days, the beat period of the synodic and anomalistic months.

A third important condition is the closeness of the moon to a node, either of two points in its orbit that lie on the ecliptic, the plane of the earth's orbit around the sun. The moon crosses the ecliptic twice every 27.2-day nodical month. Maxima in perigean tides occur when the moon is close to the ecliptic, as well as to perigee and syzygy. This happens, on average, every 2.99847 calendar years to create the perigean eclipse cycle, equal to twice the beat period of the nodical and anomalistic months. The 6-year and 9-year tidal events that tend to correlate with times of cool global temperatures (3) are synchronous with every second or third perigean eclipse cycle, respectively.

A fourth condition necessary for determining maximal tidal forcing is the closeness of the earth to perihelion, the point on the earth's elliptical orbit closest to the sun, occupied every anomalistic year of 365.2596 days. When an analysis is made to find the times when all four conditions are most closely met, the 1,800-year cycle becomes apparent as a slow progression of solar-lunar declinational differences that coincide with progressive weakening and then strengthening of successive centennial maxima in tidal forcing (Fig. 2). The 1,800-year cycle thus represents the time for the recurrence of perigean eclipses closely matched to the time of perihelion. Progressively less close matching of perigee, node, and perihelion with syzygy occur, on average, at intervals of 360, 180, 90, 18, and 9 years.

The long term average period of the 1,800-year cycle can be computed from the circumstance that the period of the perigean eclipse cycle falls 0.610061 days short of 3 anomalistic years. Independent of the condition of syzygy, the long term period is 1795.26 years ($2.99847 \times 365.2596/0.610061$), equal to the beat period of the anomalistic year with one-third of the period of the perigean eclipse cycle. The actual timing of specific maximum events of the 1,800-year cycle depends, however, also on the timing of syzygy. This additional requirement causes the intervals between specific maxima to occur at intervals of 1,682, 1,823, or 2,045 years, or even occasionally $\pm$ 18.03 years from these three principal intervals. (An example is the 1,682-year interval from A.D. 1425 to 3107, noted above.) The maxima of the centennial cycles are also irregular. The 360-year cycle has principal intervals of 345, 363, and 407 years, plus occasionally others. The 180-year cycle has a wide range of intervals, in 9-year increments, from 141 to 204 years. The 90-year tidal interval can be either 84 or 93 years.

A 5,000-Year Modulation of the 1,800-Year Cycle. A further millennial cycle arises from variability in the strengths of the maxima of the 1,800-year cycle. In the lowest plot of Fig. 3 is shown a hypothetical sequence of tidal events assuming, as a starting point, zero separation-intervals of syzygy from perigee, lunar node, and perihelion. The calculations assume that the lunar months and anomalistic year have constant periods appropriate to the present epoch. The γ value of all tidal events above a threshold of 17.150° per day are plotted. Every second or third 1,800-year maximum in γ is seen to be more prominent. The cause of this pattern can be understood by viewing the top plot of Fig. 3, which shows the separation-interval of syzygy from perihelion, in days, for all tidal events in the 360-year centennial cycle. This time-difference describes a pattern consisting of a generally declining difference interrupted by an abrupt upward shift that occurs 61 times in a simulation of 283,674 kyr (not all plotted): hence, an average period of 4,650 years.

Shown in the middle plot of Fig. 3 is the departure, in arc degrees, of the moon from the plane of the ecliptic for the same events as shown in the upper plot. This angular difference describes a similar pattern to that of the upper plot, but with the average period of the 1,800-year cycle. The separation-interval of syzygy from perigee (not shown) remains small (less than 2 hr) for all of the maximum millennial events shown in Fig. 3. Thus, the 1,800-year cycle arises from progressive mismatches of syzygy and lunar node, the 4,650-year cycle from progressive mismatches of syzygy and perihelion. These two cycles are incommensurate even though both are expressed by recurring maxima of the 1,800-year cycle.

Observational Tests of Millennial Tidal Climatic Forcing. Time-series of ice-rafted debris (IRD) from sedimentary cores in the North Atlantic ocean (1, 2), and associated temperature proxy data, show evidence of repeated rapid cooling events in the Northern

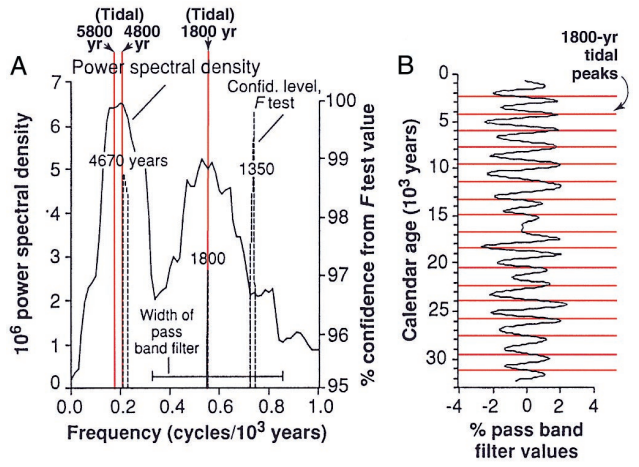

Fig. 4. Multitaper spectral analysis of glacial-Holocene petrologic events from cores VM 29–191 and VM 23–81 (reproduced from ref. 2, Fig. 7), compared with periodicities in tidal forcing. Overlain in red are the averages (calculated from 0 to 31.1 kyr BP) of the 1,800- and 5,000-year tidal periods (*A*) and times of peak forcing of the former cycle (*B*). Tidal timing and periodicity assume invariant orbital parameters, except for the 5,800-year period that is based on assuming secular variability of climatic precession, as described in the ''Secular Variations in Tidal Forcing'' section of the text.

Hemisphere, as summarized in "The 1- to 2-kyr IRD Cycle" section above. We now show, from results of both spectral analysis and direct comparisons of events, that strong oceanic tidal forcing may have occurred in association with IRD events.

Spectral analysis of the IRD records, from 1- to 31-kyr BP, reproduced in Fig. 4 from Bond *et al.* (2), show broad peaks centered at 1,800 and 4,670 years (Fig. 4*A*), in contrast to an average pacing between IRD events of 1,470 ± 532 years. The peak periods agree closely with the 1,800-year and 5,000-year tidal cycle periods, shown by added vertical red lines. Bond *et al.* (2) also determined the phasing of the 1,800-year IRD band by filtering their data with a bandpass centered at 1,800 years (Fig. 4*B*). Cold periods, indicated by high filter values, nearly coincide with 1,800-year tidal events, shown by added horizontal red lines.

A possible explanation for the disparity between the pacing of about 1,500 years, and the spectral period of about 1,800 years in the IRD data, is provided in Fig. 5 by a direct comparison of IRD cold events (dashed black lines) with times of strong tidal forcing (solid red lines). Between 0.6 and 31.2 kyr BP, 18 IRD events collectively exhibit an average spacing of 1,800 years while 4 others ("7", "YD," and one each near 14 kyr BP and 1.4 kyr BP) are spaced nearly midway between events of the first subset, 3 of these in a cluster near 12 kyr BP. The resulting bimodal pacing accounts for finding a broad spectral peak near 1,800 years, despite an average pacing of 1,470 years. Furthermore, the 1,800-year spectral peak is again found when the IRD record is extended back to 80 kyr BP (ref. 1, Fig. 8), with similar phasing of the associated bandpass. Additional clusters of events with about half the pacing of the majority again suggests a bimodal distribution in pacing (Fig. 6 in ref. 1).

A possible cause of an 1,800-year IRD cycle, consistent with tidal forcing, is the concept of "threshold behavior" of nonlinear systems suggested by Bond *et al.* (ref. 1, p. 51). Suppose that the primary mechanism of the 1- to 2-kyr IRD cycle is an unstable

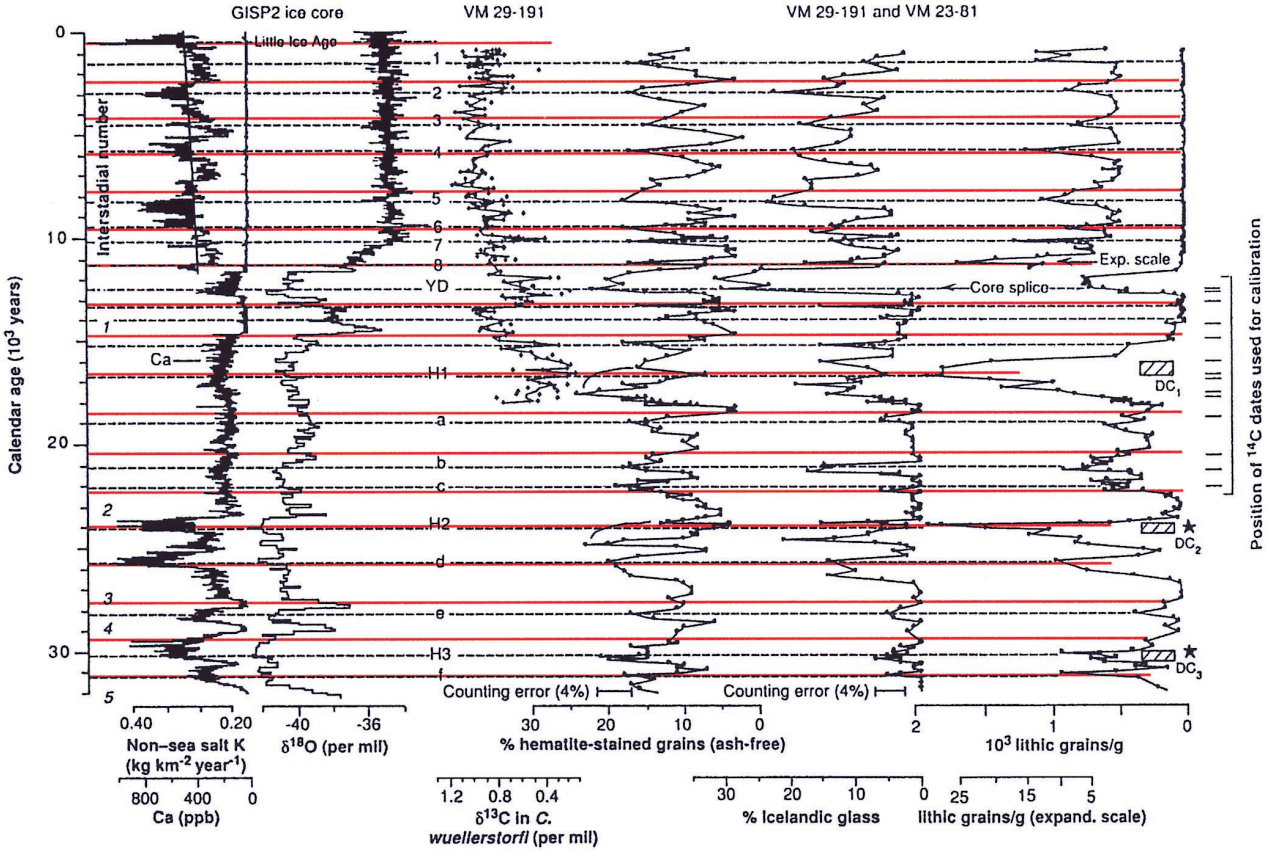

Fig. 5. Glacial-Holocene deep-sea core record of ice-rafted debris, petrology, and isotopes of the North Atlantic Ocean basin (from ref. 2, Fig. 6; BP in kyr before A.D. 1950), which shows evidence of pervasive millennial-scale fluctuations in climate. Overlaid in red are times of peak forcing in the 1,800-year tidal cycle.

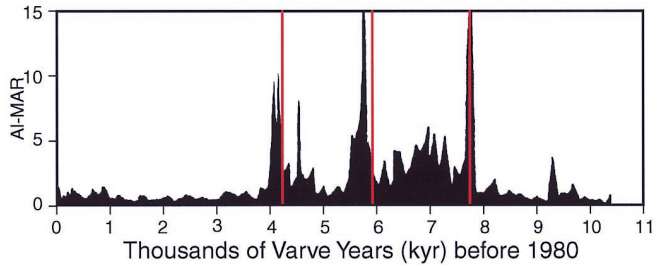

Fig. 6. Profile of mass accumulation rate of aluminum (AL-MAR in mg/cm^2/yr) in sediments of Elk Lake, Minnesota [from Dean (ref. 8, Fig. 2)]. Overlain in red are the times of peak forcing in the 1,800-year tidal cycle (at 4,239, 5,921, and 7,744 yr BP).

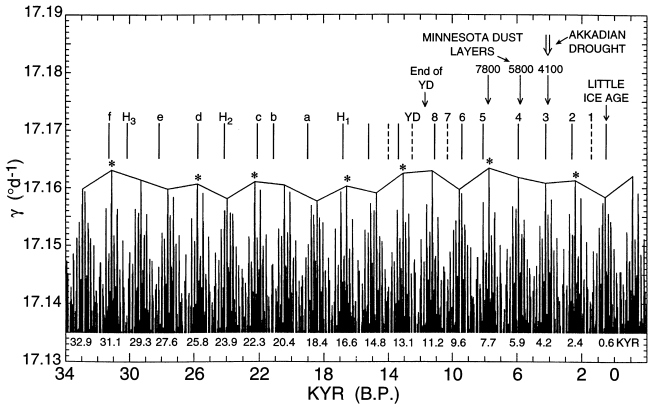

Fig. 7. Comparison of late-glacial and Holocene sedimentary core chronology of the North Atlantic Ocean basin with the times of tidal forcing. Tidal events are shown as in Figs. 1 and 2 with times of 1,800-year climactic events (in kyr BP) listed below. These climactic events are connected by line segments. Those that contribute to the 5,000-year tidal cycle are marked with asterisks. Immediately above this plot are vertical lines indicating cool periods inferred from the deep-sea core records, labeled as in Fig. 5. Their timing is derived from Fig. 5, except for Event 1 and Events 3–8, which are dates quoted in the text of ref. 2, and Event 2, inferred from Bond *et al.* (ref. 1, Fig. 14). Plotted as arrows are the times of dust layers in Elk Lake, Minnesota, the beginning of the Akkadian drought [as reported by Kerr (9)], the Little Ice Age, and the end of the Younger Dryas (YD) [Bond *et al.* (2)]. Events consistent with the hypothesis of tidal forcing of climate are shown as solid lines, exceptions as dashed lines.

system in which distinct periodic forcing is always capable of causing a threshold to be exceeded, but that the threshold is occasionally exceeded without this forcing operating. The result could be an irregular pacing of events without obliterating the evidence of a cyclic process associated with this forcing.

A handicap in establishing a cyclic character to sedimentary core data is the uncertainty in their time-scale. Records of IRD events from four separate sedimentary cores in the North Atlantic, plotted together by Bond *et al.* (ref. 1, Fig. 14) show deviations in the timing of IRD events, from one core to another, of the same order as their deviations from the times of 1,800-year tidal events. For the Holocene era, a more precise comparison of cooling and tidal events is afforded by dust layers in sediments of Elk Lake, situated near the boundary of forest and prairie in north-central United States (8). The layers, millimeter-scale annual laminations that permit high resolution calibration of climatic events ($\pm$ 200 years) back to 10 kyr BP, are believed to represent cold, dry periods in a region sensitive to climate change (8).

The three most prominent dust layers of Elk Lake (Fig. 6) are nearly coincident with 1,800-year tidal events at 4,239, 5,921, and 7,744 yr BP. Suggestive of a world-wide phenomenon, the most recent Elk Lake event, dated at 4,100 yr BP, is essentially contemporaneous with a dust spike in Peruvian Ice, dated at 4,200 $\pm$ 200 yr BP, marking a major drought in the Amazon Basin, and a dust layer, dated at 4,000 $\pm$ 100 yr BP in sediments of the Red Sea, that may have been caused by widespread drought, contributing to the collapse of Akkadia, the world's first empire (9).

We summarize the relationship of strong global tidal forcing to times of inferred cooling events in Fig. 7. The timing of dust layers, from lake sediments, and of the Little Ice Age, from historic data, correspond closely with peaks of the 1,800-year tidal cycle. If four previously identified exceptional events (dashed vertical lines) are excluded, the timing of the remaining IRD events also corresponds to peak tidal events almost within the stated uncertainty in their dating, not less than 5% (ref. 1, p. 39). The IRD event (number 5) near 8,100 yr BP is particularly noteworthy because it appears to be associated with the most abrupt and widespread climate shift known from the past 10 kyr (10); it is believed to have been initiated by a large freshwater pulse from Laurentide lakes, dated at 8,470 yr BP, that reduced surface ocean salinity in the North Atlantic Ocean, thereby causing widespread cooling near 8,200 yr BP (11). Two recently drilled sedimentary cores show multiple IRD events between 8,300 and 7,400 yr BP (ref. 1, Fig. 14). Together with the Elk Lake dust layer of 7,800 yr BP, these data suggest prolonged or repeated cooling well beyond the time expected for a freshwater discharge to directly affect climate. The maximum tidal forcing near these events at 7,744 yr BP was the greatest in 20,000 years, preceded and succeeded by strong forcing at 8,089 and 7,381 yr BP of the 360-yr tidal cycle. Thus the tidal hypothesis suggests that cooling initiated by a freshwater pulse may have been prolonged by tidal forcing. Also consistent with tidal forcing is the possibility that the timing of the freshwater pulse occurred during a warm phase of the 1,800-year tidal cycle, about 700 years before maximum forcing at 7,744 yr BP.

Secular Variations in Tidal Forcing. Over tens of millennia it is unrealistic to assume that the periods of the lunar months and the anomalistic year are constant, as we have in our calculations described so far. We have no information to determine secular variations in the lunar months, but we have recalculated γ, our measure of tidal forcing, taking account of secular variations in the time of passage of perihelion and in the eccentricity of the earth's orbit as listed in a table kindly supplied to us by A. Berger (private communication).

Variations in the anomalistic year are proportional to $P/(P - 1)$ where P denotes the period of "climatic precession," defined as the time-interval between two consecutive passages of the vernal equinoxial point at perihelion. The period of climatic precession has been estimated (12) to have varied between 19 and 28 kyr during the past 60 kyr, with the largest variations before 33 kyr BP.

When a variable anomalistic year, derived from the prescribed secular variation of P , is introduced into our calculations, the average period of the 1,800-year cycle, from 33 kyr BP to the present, is only slightly altered from 1,795 to 1,805 years. The 5,000-year modulation of this cycle is significantly lengthened, from 4,787 to 5,769 years, but is still consistent with the corresponding spectral band for IRD events (shown in Fig. 4). The magnitudes of peak tidal events of the 1,800-year cycle are almost identical back to 10 kyr BP, and the dates are identical back to 14 kyr BP. Thus our conclusions with respect to climate forcing of the Holocene should not be affected by our neglect of secular orbital variations.

Before the Holocene era the timing of peak tidal events gradually departs from that calculated, assuming a constant anomalistic year such that the 1,800-year peak occurred 123

years earlier at 33,066 yr BP, still an insignificant difference when making comparisons with events seen in core records. Variability in magnitude of the peak 5,000-year events diminishes between 16 and 33 kyr BP, during a time of rapidly changing climatic precession, suggesting that the assumption of a constant anomalistic year exaggerates variability in γ on long time-scales.

Moreover, we have noticed a similar tendency on the decadal time-scale. The plotted arcs of the 18.03-year Saros cycles, shown in Fig. 1, based on accurate orbital data, are more regular than those plotted in Fig. 2, based on assuming constant lunar months. The irregularities that we find in tidal strength and timing over longer periods might further decrease if we prescribed more exact motions of the moon and earth, as well as prescribing variable climatic precession.

[A cause for such greater regularity in tidal forcing might be resonances of other bodies of the solar system, especially the outer planets. We are struck by the close correspondence of the average period of the 180-year tidal cycle of 179.5 years (1/10 of that of the 1,800-year cycle) and the period of the sun's rotation about the center of mass of the solar system of 179.2 years, the latter a manifestation of planetary resonances (13).]

We have also calculated the effect on γ of varying eccentricity. First, we estimated the variation of γ with distance, R , of the earth from the sun by establishing the average seasonal cycle of γ derivable from the data of Wood (ref. 5, Table 16). We then assumed a dependence proportional to R^3 for both the seasonal and secular rate of change in R. The 1,800-year cycle in γ remains almost exactly as at constant eccentricity, but a 100-kyr variation is introduced into γ that is several times as large as the amplitude of the 1,800-year cycle. We tentatively conclude that, although varying eccentricity strongly affects tidal forcing, and could possibly contribute to the 100-kyr cycle of glaciation, it has little influence on the cycles under discussion here.

Ramifications of the Tidal Hypothesis. The details of the tidal hypothesis are complex. There is much about tidal forcing that we do not know, and there is not space here to discuss all that we do know that could contribute to proving whether it is the underlying cause of some, or all, of the events of rapid climate change. We are convinced, however, that, if the hypothesis is to a considerable degree valid, the consequences to our understanding of the ice-ages, and of possible future climates, are far from trivial.

Should the tidal hypothesis of quasi-periodic cooling of the oceans turn out to be correct, a prevailing view that the earth's postglacial climate responds mainly to random and unpredictable processes would be modified or abandoned. The 1,800-year tidal cycle would be recognized as a principal driver of climate change in the Holocene, causing shifts in climate more prominent and extensive than hitherto realized. The Little Ice Age would be seen to be only a lesser cooling episode in a series of such episodes. Viewed today as of "possibly global significance" (14), it would probably be confirmed as such, being linked to global tidal forcing. Other major climatic events since the glacial period, such as drought near the time of collapse of the Akkadian empire, might also be found to be linked to a global process.

Looking ahead, a prediction of "pronounced global warming" over the next few decades by Broecker (15), presumed to be triggered by the warm phase of an 80-year climatic cycle of unidentified origin, would be reinterpreted as the continuation of natural warming in roughly centennial increments that began at the end of the Little Ice Age, and will continue in spurts for several hundred years. Even without further warming brought about by increasing concentrations of greenhouse gases, this natural warming at its greatest intensity would be expected to exceed any that has occurred since the first millennium of the Christian era, as the 1,800-year tidal cycle progresses from climactic cooling during the 15th century to the next such episode in the 32nd century.

We thank Gerard Bond for numerous helpful discussions and André Berger for advice on the astronomical tides and valuable astronomical data. We also thank David Cartwright, Christopher Charles, Walter Dean, Devandra Lal, Walter Munk, and Jeff Severinghaus for advice on climate change and tidal theory. We are especially indebted to Fergus Wood for pointing out to us that the function γ would serve to indicate the strength of tidal forcing. We owe much to his having tabulated γ over more than 500 years. It was the curious progressive increase in γ from Event D to Event A of Fig. 1, suggestive of a millennial periodicity, that led us to discover the 1,800-year tidal cycle. Financial support was provided by the National Science Foundation (Grant ATM-97-11882) and the U.S. Department of Energy (Grant FG03-95ER-62075).

1. Bond, G., Showers, W., Elliot, M., Evans, M., Lotti, R., Hajdas, I., Bonani, G. & Johnson, S. (1999) *Mechanisms of Global Climate Change at Millennial Time Scales* (Geophys. Monog. 112, Am. Geophys. Union, Washington, DC), pp. 35–59.
2. Bond, G., Showers, W., Cheseby, M., Lotti, R., Almasi, P., deMenocal, P., Priore, P., Cullen, H., Hajdas, I. & Bonani, G. (1997) *Science* **278,** 1257–1266.
3. Keeling, C. D. & Whorf, T. P. (1997) *Proc. Natl. Acad. Sci. USA* **94,** 8321–8328.
4. Munk, W. & Wunsch, C. (1998) *Deep Sea Res.* **I45,** 1977–2010.
5. Wood, F. J. (1986) *Tidal Dynamics* (Reidel, Dordrecht, the Netherlands).
6. Lamb, H. H. (1972) *Climate: Present, Past, and Future* (Methuen, London).
7. Cartwright, D. E. (1974) *Nature (London)* **248,** 656–657.
8. Dean, W. E. (1997) *Geology* **25,** 331–334.
9. Kerr, R. A. (1998) *Science* **279,** 325–326.
10. Alley, R. B., Mayewski, P. A., Sowers, T., Stuiver, M., Taylor, K. C. & Clark, P. V. (1997) *Geology* **25,** 483–486.
11. Barber, D. C., Dyke, A., Hillaire-Marcel, C., Jennings, A. E., Andrews, J. T., Kerwin, M. W., Bilodeau, G., McNeely, R., Southon, J., Morehead, M. D., *et al*. (1999) *Nature (London)* **400,** 344–348.
12. Berger, A. & Loutre, M. F. (1997) *Science* **278,** 1476–1478.
13. Herman, J. R. & Goldberg, R. A. (1985) *Sun, Weather, and Climate* (Dover, New York).
14. Jones, P. D. & Bradley, R. S, (1992) in *Climate Since A. D. 1500*, eds. Bradley, R. S. & Jones P. D. (Routledge, London), pp. 649–665.
15. Broecker, W. S. (1975) *Science* **189,** 460–463.